JOURNAL OF VIROLOGY, Nov. 2003, p. 11332–11346 Vol. 77, No. 21
0022-538X/03/$08.00+0 DOI: 10.1128/JVI.77.21.11332–11346.2003
Copyright © 2003, American Society for Microbiology. All Rights Reserved.

Measles Virus (MV) Nucleoprotein Binds to a Novel Cell Surface Receptor Distinct from FcγRII via Its C-Terminal Domain: Role in MV-Induced Immunosuppression

David Laine,[1] Marie-Claude Trescol-Biémont,[1] Sonia Longhi,[2] Geneviève Libeau,[3] Julien C. Marie,[1]† Pierre-Olivier Vidalain,[1] Olga Azocar,[1] Adama Diallo,[4] Bruno Canard,[2] Chantal Rabourdin-Combe,[1] and Hélène Valentin[1]*

Laboratoire d'Immunobiologie Fondamentale et Clinique, INSERM U503, IFR128 BioSciences Lyon-Gerland, 69365 Lyon Cedex 07,[1] Architecture et Fonction des Macromolécules Biologiques, UMR 6098,CNRS et Universités d'Aix-Marseille, 13288 Marseille,[2] and Programme Santé Animale, CIRAD/EMVT, 34398 Montpellier Cedex 5,[3] France, and Animal Production Unit, Agriculture and Biotechnology Laboratory, IAEA Laboratories, A-2444 Seibersdorf, Austria[4]

Received 19 February 2003/Accepted 22 July 2003

During acute measles virus (MV) infection, an efficient immune response occurs, followed by a transient but profound immunosuppression. MV nucleoprotein (MV-N) has been reported to induce both cellular and humoral immune responses and paradoxically to account for immunosuppression. Thus far, this latter activity has been attributed to MV-N binding to human and murine FcγRII. Here, we show that apoptosis of MV-infected human thymic epithelial cells (TEC) allows the release of MV-N in the extracellular compartment. This extracellular N is then able to bind either to MV-infected or uninfected TEC. We show that recombinant MV-N specifically binds to a membrane protein receptor, different from FcγRII, highly expressed on the cell surface of TEC. This new receptor is referred to as nucleoprotein receptor (NR). In addition, different Ns from other MV-related morbilliviruses can also bind to FcγRII and/or NR. We show that the region of MV-N responsible for binding to NR maps to the C-terminal fragment (N_{TAIL}). Binding of MV-N to NR on TEC triggers sustained calcium influx and inhibits spontaneous cell proliferation by arresting cells in the G_0 and G_1 phases of the cell cycle. Finally, MV-N binds to both constitutively expressed NR on a large spectrum of cells from different species and to human activated T cells, leading to suppression of their proliferation. These results provide evidence that MV-N, after release in the extracellular compartment, binds to NR and thereby plays a role in MV-induced immunosuppression.

Morbilliviruses cause severe diseases in humans and animals (3, 27, 63). Most of these infections are associated with the development of a transient but strong immunosuppression that contributes to secondary infections and mortality (18, 27, 63). The *Morbillivirus* genus includes *Measles virus* (MV), *Canine distemper virus* (CDV), *Rinderpest virus* (RPV), *Peste-des-petits ruminants virus* (PPRV), *Porcine distemper virus*, *Dolphin morbillivirus*, and *Porpoise morbillivirus*. The nonsegmented, single-stranded, negative-sense RNA genome of morbilliviruses encodes six structural proteins. While hemagglutinin (H) and fusion (F) are external glycoproteins, the nucleoprotein (N), the phosphoprotein (P), the viral polymerase (L) and the matrix protein (M) are internal proteins. The P cistron also encodes the nonstructural V and C proteins, but their function is still to be clearly determined.

N packs the RNA genome to form a helical nucleocapsid (NC), which binds P and L proteins. The result of this association, the ribonucleoproteic complex, constitutes the template for the transcription and replication of the viral genome. However, N has also the ability to self-assemble onto cellular RNA in the absence of viral RNA and viral proteins (4, 25).

MV-N consists of two regions: an N-terminal moiety, N_{CORE}, and a C-terminal moiety, N_{TAIL}, which is intrinsically disordered and protrudes from the viral NC surface (21, 32). While N_{CORE} (amino acids [aa] 1 to 400) has sequences required for N self-assembly and RNA binding (2, 9, 25, 31), N_{TAIL} (aa 401 to 525) contains the regions responsible for the binding of both assembled and monomeric forms of N to P, as well as those involved in binding to the polymerase complex (P-L) (2, 19, 31). N interaction with intracellular partners relies also on N_{TAIL}: in particular, the region of MV-N encompassing residues 415 to 523 binds to the interferon regulatory factor 3, leading to the activation of the alpha/beta interferon enhancer (54). A conserved, hydrophobic patch at the extreme C terminus of MV-N binds to the heat shock protein Hsp72, which modulates the level of viral RNA synthesis (66). Despite the fact that MV-N is not exposed at the surface of the virion and of infected cells, it interacts with an extracellular receptor (45).

During the acute phase of MV infection, both strong humoral and cellular anti-N immune responses have been described. At the onset of the rash, the humoral response occurs after B lymphocyte stimulation by accessible and native MV antigens. Notably, the most abundant and rapidly produced antibodies are N specific. The production of anti-N antibodies

* Corresponding author. Mailing address: Laboratoire d'Immunobiologie Fondamentale et Clinique, INSERM U503, 21 Avenue Tony Garnier, 69365 Lyon Cedex 07, France. Phone: (33) 4-37-28-23-77. Fax: (33) 4-37-28-23-41. E-mail: valentin@cervi-lyon.inserm.fr.

† Present address: Department of Immunology, University of Washington, Seattle, WA 98195-7370.

precedes that of anti-H, anti-F, and sometimes anti-M antibodies (17, 36). These observations suggest that MV-N is released from MV-infected cells in the extracellular compartment, thus becoming accessible to the B-cell receptor. Moreover, efficient helper $CD4^+$-T and cytotoxic $CD8^+$-T-cell responses against N are generated during the course of MV infection (23, 24, 59). MV-N induces, in the absence of other viral proteins, N-specific T-cell responses, a systemic anti-N antibody response, and protection against MV infection (12, 39). Thus, MV infection is associated with an effective N-specific response that leads, with other events, to viral clearance, recovery from disease in 2 weeks, and to a protective immune response against reinfection. Paradoxically, MV simultaneously induces an immunosuppression by indirect mechanisms occurring in uninfected cells. In addition to MV H and F, experimental evidences indicate that MV-N is also involved in MV-induced immunosuppression. Indeed, MV-N binds to human and murine cell surface Fc receptor for immunoglobulin G (IgG) of type II (FcγRII, CD32) (45) and suppresses the inflammatory immune response in vivo in a murine delayed-type hypersensitivity model (34). This inhibition is associated with an inhibition of the antigen-specific $CD8^+$-T-cell proliferation and a decrease of interleukin-12 (IL-12) production by murine dendritic cells (DC) (34). MV-N also inhibits in vitro IL-12 and antibody production in human CD40-activated DC and activated B lymphocytes, respectively (45, 53).

Here, we show that MV-N is released in the extracellular compartment after apoptosis of MV-infected human thymic epithelial cells (TEC). We report that MV-N can subsequently bind to cell surface via the interaction of N_{TAIL} with a specific receptor. We call this unidentified protein the nucleoprotein receptor (NR). We demonstrate that NR binds to other *Morbillivirus*-Ns but not that of the rabies virus (RV), a member of the *Rhabdovirus* genus. Moreover, NR induces sustained calcium influx and inhibits both spontaneous and activated cell proliferation when triggered by MV-N. These results suggest that, in addition to MV-H and -F proteins, MV-N released in the extracellular compartment is involved in MV-induced suppression of cell proliferation.

MATERIALS AND METHODS

Cell lines and purification of primary cells. The P1.4D6 cortical TEC clone from human postnatal thymus was kindly provided by M. L. Toribio (13). The cell lines 3D1 (murine cortical TEC), HeLa (epithelial human carcinoma from cervix), MeWo (fibroblastic human melanoma from lymph node), NIH 3T3 (mouse fibroblasts from embryo), Jurkat (human acute T-cell leukemia), and Vero (monkey fibroblast from kidney) were obtained from the American Type Culture Collection (Manassas, Va.). The cell lines IIA1.6 (mouse B lymphoma, an FcγRII-negative variant of A20/2J cell line) and IIA1.6, expressing human FcγRIIb1 isoform (IIA1.6 Hu FcγRIIb1), were a gift from J. G. J. Van de Winkel (60). Cell lines were grown in RPMI 1640 or Dulbecco modified Eagle medium (Invitrogen, Inc., Grand Island, N.Y.) supplemented with 2 mM L-glutamine (Invitrogen), 10 mM HEPES (Invitrogen), 40 μg of gentamicin (Schering-Plough)/ml, 50 μM 2-mercaptoethanol (Sigma) (for murine and monkey cell lines), and 5 to 10% fetal calf serum (FCS) (Biomedia).

Human T cells, monocytes, and DC were purified as previously described (14). Murine T and B cells were obtained from spleen. Murine macrophages were obtained after biogel dorsal injection, and DC were obtained from lymph node as described elsewhere (33). C57BL/6 mice were purchased from IFFA CREDO (l'Arbresle, France). Gene-targeted mice lacking FcγRIII, FcγRI, and FcγRIIB (Fcer1g/Fcgr2 double-knockout mice, model 585-MM) were obtained from Taconic.

Human T-cell activation. Freshly isolated T cells were activated at 10^6 cell/ml with a combination of 10 ng of phorbol myristate acetate (Sigma)/ml and 1 μg of ionomycin (Sigma)/ml in complete culture medium (RPMI 1640 × 10% fetal calf serum), as previously described (14). After 16 h of activation, T cells were washed and used for MV-N binding and functional assays.

Antibodies. The monoclonal antibodies (MAbs) used for the detection of *Morbillivirus*-N were biotinylated anti-MV-N Cl25 (IgG2b isotype), anti-MV-N Cl120 (IgG2b isotype) (16), anti-PPRV-N 38.4 (IgG1 isotype), anti-RPV-N IVB2-4 (IgG1 isotype), and anti-RPV-N 33.4 (IgG1 isotype) (28). C. Kai (Tokyo, Japan) and M. Lafon (Paris, France) kindly provided anti-CDV-N (clone 5) and biotinylated anti-RV-N PVA3 (29), respectively. The blocking rat MAb 2.4G2, recognizing murine FcγRII (CD32) and FcγRIII (CD16) (57), and the blocking mouse MAb KB61, recognizing all human FcγRII isoforms (CD32), were kindly provided by D. Y. Mason (42). Phycoerythrin (PE) anti-human CD32 (Marseille, France), and anti-mouse CD16/CD32 (Pharmingen, San Diego, Calif.) MAbs were used. Mouse T and B cells, macrophages, and DC were visualized by using fluorescein isothiocyanate (FITC)-labeled anti-mouse CD3 (2C11, homemade), IgG [goat $F(ab')_2$ fragment mouse IgG], IgG-FITC (Immunotech), CD11b (Immunotech), and CD11c (Pharmingen) MAbs, respectively. Rat and mouse IgG1 and IgG2 isotypic controls (Immunotech) were used as isotypic controls of immunofluorescence.

Cl25 MAb was adsorbed on polystyrene microparticles according to the manufacturer's instructions (Polysciences). Briefly, 0.5 ml of bead suspension was washed in borate buffer prior to incubation with 400 μg of Cl25 MAb overnight at room temperature. Beads were then extensively washed and stored at 4°C in 5% glycerol storage buffer. MAb adsorption on beads was then confirmed by flow cytometry with PE-conjugated goat anti-mouse IgG (Immunotech).

Cloning, production, and purification of *Morbillivirus*-N and RV-N. Viral MV-N was produced from Vero cells infected with MV Hallé strain at 0.01 PFU/cell as described previously (45). Recombinant MV-N was produced from confluent Sf9 cells infected with recombinant baculovirus AcNPVNP at 1 PFU/cell, as previously described (45). The PPRV gene (Nigeria 75/1 vaccine strain) (10) was subcloned into the plasmid pAcYM1 under the control of the polyhedrin promoter and transferred into the baculovirus AcNPVNP by homologous recombination in transfected insect cells. Recombinant PPRV was produced in insect Sf9 cells (30). For the rinderpest N protein (RPV-N), the coding sequence of the N protein gene (RGK1 strain) was amplified by reverse transcription-PCR and cloned into the transfer vector pBacPAK9 (Clontech) downstream of the polyhedrin promoter. The final plasmid was used to generate the recombinant baculovirus RGK1-N by cotransfection of Sf9 cells with the *Bsu*36 I-digested BacPAK6 viral DNA (Clontech). The gene encoding CDV-N from M13mp19 CDVNP (kindly provided by R. Buckland, Lyon, France) was cloned into the *Bam*HI site of pFASTBac 1 (Invitrogen). Baculovirus CDV-N was prepared according to the instruction manual of Bac-To-Bac baculovirus expression system (Invitrogen). The recombinant baculovirus RV-N was a gift from M. Lafon (Paris, France), and the corresponding cDNA was constructed as described previously (41). Sf9 cells were infected with RPV-N, PPRV-N, CDV-N, or RV-N recombinant baculoviruses at a multiplicity of infection of 1. Cells infected with MV or recombinant baculoviruses were lysed, and viral N or recombinant-N was purified on a preformed gradient of 50 to 30 to 25% (wt/vol) CsCl and 5% sucrose (wt/vol) as previously described (45).

Recombinant MV-N was also obtained from *Escherichia coli* as described elsewhere (25). The N_{CORE} fragment, corresponding to aa 1 to 400 of MV-N, was obtained by limited proteolysis of purified N as described by Karlin et al. (25). The gene fragment of MV-N coding for N_{TAIL} (residues 401 to 525) was cloned into the pQE-32 vector (Qiagen), which allows the bacterial expression of a hexahistidine-tagged recombinant product. Protein expression was performed as described previously (32). The protein was purified by immobilized metal affinity chromatography by using ni-nitrilotriacetic acid agarose (Qiagen). The identity of the purified product was confirmed by Western blotting with an anti-hexahistidine tag MAb from Qiagen (data not shown). Purified *Morbillivirus*-Ns were solubilized in phosphate-buffered saline (PBS) or in TNE buffer (20 mM Tris-HCl, 50 mM NaCl, 2 mM EDTA; pH 8) containing 20% glycerol. For functional assays, N preparations were dialyzed against TNE buffer to remove glycerol.

All virus stocks were free of mycoplasma.

MV infection and detection of N in cell-free supernatants by ELISA. TEC were seeded at 5×10^3 cells/cm^2 for 24 h and then infected at a multiplicity of infection of 0.1 with Vero cell-derived MV strains for 2 h. MV strains were parental recombinant MV-Tag (derived from Edmonston strain) or MV-Tag defective for V or C expression (MV-V^- or MV-C^-) (43, 44, 50). After extensive washes, TEC were treated or not with 10 μg of the fusion-inhibiting peptide (FIP) Z-D-Phe-L-Phe-Gly-OH/ml (46), kindly provided by D. Gerlier (Lyon,

France). At different times postinfection, cell-free supernatants were collected for enzyme-linked immunosorbent assays (ELISAs) and for infectious MV particle production. The median 50% tissue culture infective dose ($TCID_{50}$) was calculated as previously described (61). For ELISA assays, cell-free supernatants were UV inactivated (30 min at 254 nm) and twofold serially diluted. The N content was then measured by capture ELISA as described elsewhere (34). A reference MV-N curve was established by using serial dilutions of purified viral MV-N. MV-N purified on a sucrose gradient was used as an internal control to demonstrate that only free N and not virion-associated MV-N was measured in our ELISA conditions.

Cell viability and apoptosis analyses. $DIOC_6(3)$ (3,3′-diexyloxacarbocyanine; Molecular Probes, Inc., Eugene, Oreg.) and propidium iodide (PI) double staining was performed to detect the viability and mortality of TEC cultures by flow cytometry. Briefly, cells were incubated for 15 min at 37°C with 40 nM $DIOC_6(3)$ in culture medium to evaluate mitochondrial transmembrane potential ($\Delta\psi_m$) (58). As $\Delta\psi_m$ decreases with cell commitment to apoptosis, $DIOC_6(3)$ stains living cells but not apoptotic cells. PI (0.5 μg/ml) was added before flow cytometry analysis by using a calibur flow cytometer and CellQuest software (Becton Dickinson). Integrated fluorescence was measured, and data were collected from at least 2 min.

TEC apoptosis was also assayed by using an FITC (Sigma) conjugate of the cell-permeable caspase inhibitor VAD-FMK (Promega, Madison, Wis.). Upon entry of the inhibitor into the cells, it irreversibly binds to activated caspases and thus serves as a specific in situ marker for apoptosis. Attached and floating cells were pooled and incubated 20 min at room temperature in the presence of FITC-VAD-FMK at 5 μM. Cells were then washed twice, and FITC-VAD-FMK labeling was determined by flow cytometry. Integrated fluorescence was measured, and data were collected for at least 1 min. For the assessment of nuclear features of apoptosis, MV-infected TEC were stained with Hoechst 33342 (10 μg/ml; Sigma) for 30 min at 37°C as previously described (58).

Detection of FcγRII. For cell surface detection of human FcγRII (CD32) or mouse FcγRII/III (CD32/CD16), direct immunofluorescence assays were performed for 30 min at 4°C in staining buffer (PBS containing 1% bovine serum albumin and 0.1% sodium azide) with PE-conjugated anti-FcγRII±III MAbs. After labeling, cells were analyzed by flow cytometry analysis. Integrated fluorescence was measured, and data were collected from at least 10,000 events.

Detection of *Morbillivirus*-N binding by flow cytometry. To determine *Morbillivirus*-N, MV-N_{CORE}, or MV-N_{TAIL} binding to cells, 5×10^5 cells were incubated for 1 h at 4°C with 100 μl of purified N (50 μg/ml) in the presence or in the absence of blocking anti-FcγRII MAb in staining buffer. After three washes, cells were incubated for 30 min at 4°C with biotinylated MAbs specific for MV-, PPRV-, and RPV-N. Cells were then incubated with streptavidin-PE (Caltag Laboratories, Santa Cruz, Calif.) for 30 min at 4°C. For CDV-N binding assays, anti-CDV-N (clone 5) and PE-conjugated goat anti-mouse IgG were used. Labeled cells were analyzed by flow cytometry as previously described. The mean fluorescence intensity (MFI) value was determined to quantify N binding. For inhibitory binding assays, the MFI obtained in the absence of human or murine anti-FcγRII±III MAbs was considered 0% inhibition.

For dual immunofluorescence labeling, murine T cells, B cells, macrophages, and DC were first incubated with 2C11-FITC, anti-IgG-FITC, CD11b-FITC, and CD11c-FITC MAbs, respectively, and this step was followed by MV-N incubation in the presence or absence of the blocking 2.4G2 MAb, as described above.

Protease and cycloheximide treatment of TEC. Cells were resuspended at a concentration to 10^6 cells/ml in RPMI 1640 without FCS and incubated at either 37°C for 30 min with 1 mg of pronase or 2 mg of trypsin/ml or at 37°C for 1 h with 100 μg of papain/ml (all enzymes were from Boehringer Mannheim). TEC were then washed three times and resuspended in RPMI 1640. The MV-N binding assay was then performed as described above.

To study the regeneration of MV-N-binding activity, protease-treated TEC were resuspended in RPMI 1640 containing either 6% FCS alone or 10 μg of cycloheximide/ml, followed by incubation at 37°C for 4 h prior to the MV-N binding assay.

Competition of MV-N binding by flow cytometry. FITC was solubilized in 1 mg of sodium carbonate-bicarbonate buffer/ml according to the manufacturer's instructions (Sigma). Recombinant MV-N was dialyzed prior to labeling against NaCl (0.15 M) for 24 h. MV-N was incubated with soluble FITC (35 μl/mg of MV-N) for 2 h at 4°C in the dark. FITC-labeled MV-N (FITC-MV-N) was dialyzed against PBS for 72 h to remove FITC excess. Based on the assumption that the MV-N concentration was not affected by FITC labeling, increasing concentrations of FITC-MV-N were applied to TEC for N binding assays. Cells were then analyzed by flow cytometry. For competition experiments, 100 μl of FITC-MV-N (25 μg/ml) was incubated with various amounts of unlabeled MV-N. The MFI obtained with FITC-MV-N alone was considered 100%.

Competition experiments were also performed with N_{TAIL} or N_{CORE} as a competitor. A 2.5-μg portion (25 μg/ml) of MV-N was incubated with increasing amounts of either N_{CORE} or N_{TAIL} for 1 h at 4°C. Cells were then incubated with biotinylated anti-N Cl25 or anti-N Cl120 MAbs, respectively, followed by streptavidin-PE incubation. The MFI was measured, and the percentage of inhibition of MV-N binding was calculated.

Immunofluorescence confocal microscopy. A total of 5×10^5 TEC were incubated for 1 h at either 4°C or 37°C with 100 μl of 50 μg of purified FITC-MV-N/ml. Then, the TEC were fixed for 20 min at 4°C in fixation buffer (2% paraformaldehyde–PBS). After extensive washes with staining buffer, cells were analyzed by confocal microscopy (Zeiss Axioplan 2 and an X63 objective lens, with laser excitation at 488 nm) to determine MV-N internalization.

Calcium mobilization assays. For intracellular Ca^{2+} mobilization, TEC were loaded at a final concentration of 10^7/ml in culture medium without FCS containing indo-1 (4 μM) and pluronic F-127 (0.08%) (Molecular Probes). Loading was conducted at 37°C for 45 min in the dark. TEC were then washed and recovered in PBS containing 1% FCS. Flurorescence was analyzed with a Kontron (Zurich, Switzerland) SFM 25 spectrofluorometer by using 350- and 405-nm wavelengths for excitation and emission, respectively (48).

Cell proliferation and cell cycle analyses. TEC were seeded in triplicate at 10^4 cells/well in a 96-well plate for 24 h before incubation with various amounts of either recombinant MV-N or N_{CORE} or N_{TAIL}. For TEC treated with N_{TAIL}, Cl25 MAbs adsorbed on beads were added at a concentration of two beads per cells. After 12 h of TEC treatment, 0.5 μCi of [^{3}H]thymidine (Perkin-Elmer)/well was added. After 24 h, cells were harvested onto a glass fiber filter (Packard) and counted by using a direct beta counter (Matrix; Packard).

Activated T cells were seeded in triplicate at 10^6 cells/ml in a 96-well plate and cultured with various amounts of MV-N either immediately or 24 to 48 h later. After 16 h of T-cell treatment, 0.5 μCi of [^{3}H]thymidine was added/well and, 8 h later, the cells were harvested and counted by using a direct beta counter.

For cell cycle analysis, DNA/RNA staining was performed by using 7-aminoactinomycin D (7AAD) and pyronin Y (PY), respectively, as previously described (55). Briefly, unfixed (5×10^5) TEC were suspended in 1 ml of nucleic acid staining solution (0.15 M NaCl in 0.1 M phosphate citrate buffer containing 5 mM EDTA and 0.5% bovine serum albumin [pH 6]). Then, 50 μl of 400 μM 7AAD (Sigma; final concentration, 20 μM) was added, followed by incubation for 30 min at room temperature. The cells were then cooled on ice. After 5 min, 50 μl of 10 μM PY (Molecular Probes; final concentration, 0.5 μM) was added, and the cells were incubated for at least 3 min on ice. The cells were then analyzed by flow cytometry. The data were collected from at least 50,000 events.

RESULTS

Extracellular N release is associated with MV-induced apoptosis. Although N is commonly considered an internal protein, the abundant production of anti-N antibodies in the course of MV infection strongly suggests that N is released from MV-infected cells, a possibility that we investigated. We used MV strains having different cytopathic activities (11) and a human TEC model in which apoptosis is dependent on MV replication (58). We first compared the ability of Tag/Edm, MV-V^-, and MV-C^- strains to propagate in TEC. As illustrated in Fig. 1A, large syncytia were observed in Tag/Edm- and MV-V^--infected TEC at day 5 postinfection. Twenty to 30% of cells died of apoptosis (Fig. 1A), as assessed by caspase activation, blue trypan coloration, and Hoechst staining (data not shown). In contrast, MV-C^- infection induced a moderate cytopathic effect, with small syncytia and a very low level of apoptosis (9.6%, Fig. 1A). Moreover, we observed efficient production of viral particles by TEC infected with Tag/Edm and MV-V^- compared to TEC infected with MV-C^- (Fig. 1A). We then analyzed the ability of these strains to release N in the cell-free supernatant by ELISA. As shown in Fig. 1B, high amounts of N were detected in cell-free culture supernatants of Tag/Edm and MV-V^--infected TEC, reaching up to 12 μg/ml on day 5. In contrast, MV-N was not detected in the cell-free culture supernatants of MV-C^--infected TEC, sug-

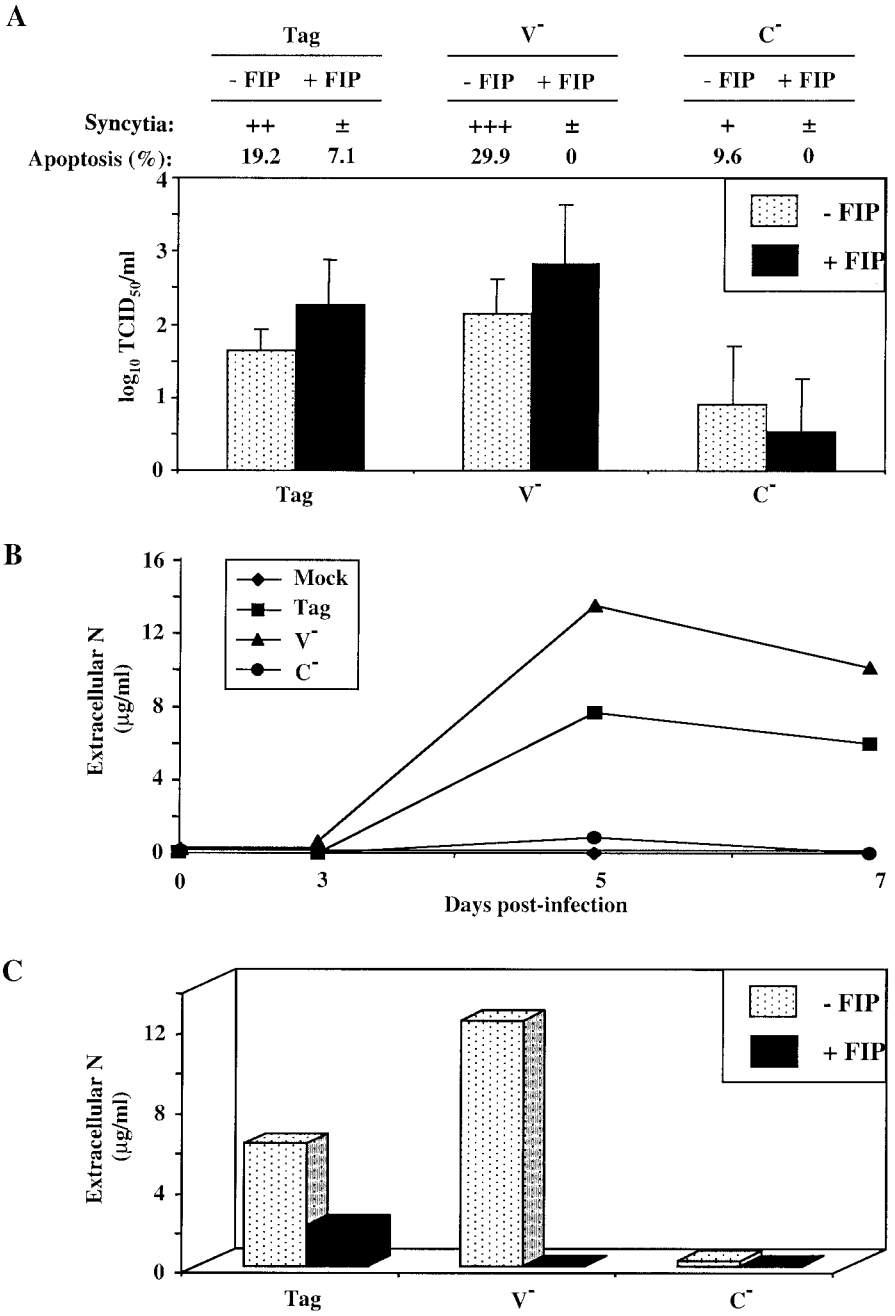

FIG. 1. Extracellular MV-N release after apoptosis of MV-infected cells. TEC were infected with recombinant MV Tag/Edm, MV-V⁻, or MV-C⁻ and then treated with or without the FIP Z-D-Phe-L-Phe-Gly-OH. (A) Inhibition of MV-induced cytopathic effect in TEC by FIP on day 5. Attached TEC were visualized by May-Grunwald–Giemsa staining, and syncytium formation was determined under light microscope. ±, +, ++, and +++, relative intensities of the cytopathic effect as defined by the number and the size of the syncytia. The percentage of pooled attached and floating TEC was evaluated by measuring caspase activity by flow cytometry. The number of infectious virus particles produced ($TCID_{50}$/milliliter) is expressed as the mean ± the standard deviation (SD) of three different experiments. (B) Time course determination of extracellular N release in MV-infected TEC culture supernatants. Samples were prepared and assayed by ELISA as described in Materials and Methods. N concentrations were evaluated with known amounts of standard purified viral MV-N. (C) Inhibition of extracellular N release by FIP on day 5. The experiments were performed twice, and SD values were <10%.

gesting that extracellular N release is dependent either on apoptosis of infected TEC or on the presence of MV-C protein.

Relationships between MV-induced apoptosis and N release are also supported by experiments performed with a FIP known to inhibit "cell-to-cell" virus spreading. As illustrated in Fig. 1A, FIP inhibited both syncytium formation and apoptosis in MV-infected TEC (93 to 100% of inhibition) but had no effect on virus particle production. Moreover, FIP inhibited MV-N release in culture supernatants on day 5 postinfection

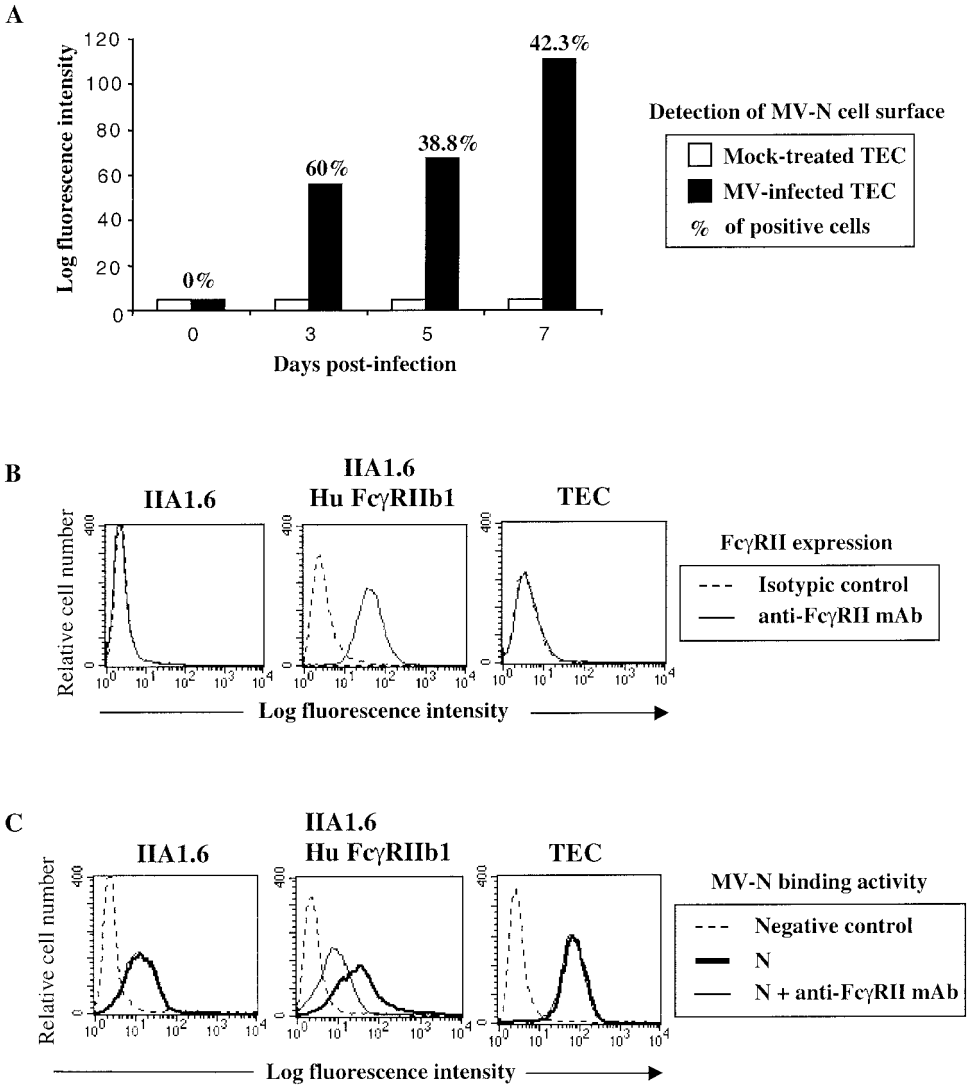

FIG. 2. Binding of MV-N to cells expressing FcγRII and another cell surface receptor. (A) Cell surface expression of N on living MV-infected TEC. TEC were infected with Edmonston MV strain at 0.1 PFU/cell. At different times postinfection, MV-N cell surface detection was determined by flow cytometry analysis with anti-MV-N (Cl25) and streptavidin-PE. The results are representative of six different experiments. (B) FcγRII expression on murine IIA1.6, on IIA1.6 expressing human FcγRIIb1, and on human TEC cell lines was detected by using anti-CD32-PE. For IIA1.6 and TEC, isotypic control and anti-CD32-PE are totally superimposed. (C) MV-N binding was detected with specific biotinylated anti-MV-N (Cl25) and then revealed with streptavidin-PE prior to flow cytometry analysis. Cells were incubated with 5 μg of purified recombinant MV-N in the absence (heavy line) or in the presence (thin line) of human blocking KB61 MAb. As a negative control, cells were incubated without MV-N in the presence of anti-MV-N (Cl25) and streptavidin-PE (dotted line). For IIA1.6 and TEC, the fluorescence intensity obtained in the presence of KB61 MAb superimposes on that obtained in the absence of this MAb. The results are representative from one of three independent experiments.

(Fig. 1C), showing a correlation between apoptosis of MV-infected TEC and N release in the extracellular compartment. As a result, N becomes accessible to cell surface receptors.

MV-N binds to cells expressing or lacking FcγRII. To determine whether released N is capable of binding to the cell surface, living MV-infected TEC were assessed for MV-N cell surface detection by using a biotinylated anti-N MAb (Cl25) and streptavidin-PE. As shown in Fig. 2A, MV-N on the TEC cell surface was detected from 3 to 7 days postinfection, indicating that, after N release, MV-N binds to neighboring cells. To further study the ability of N to bind to TEC, we used both recombinant MV-N purified from insect cells and viral MV-N purified from MV-infected Vero cells. Murine IIA1.6 and human TEC cell lines, both negative for the expression of FcγRII (CD32), as well as a murine IIA1.6 cell line expressing the human FcγRIIb1 (IIA1.6 Hu FcγRIIb1), were used (Fig. 2B). TEC also failed to express both FcγRI (CD64) and FcγRIII (CD16) (data not shown). All of these cell lines, expressing or not expressing FcγRII, efficiently bound recombinant and viral MV-N (Fig. 2C and data not shown). MV-N binding to IIA1.6 and TEC was not affected by blocking anti-FcγRII MAb, indicating that MV-N binding does not occur through FcγRII (Fig. 2C). In contrast, the addition of blocking anti-FcγRII MAb partially inhibited (50 to 65% of inhibition) MV-N bind-

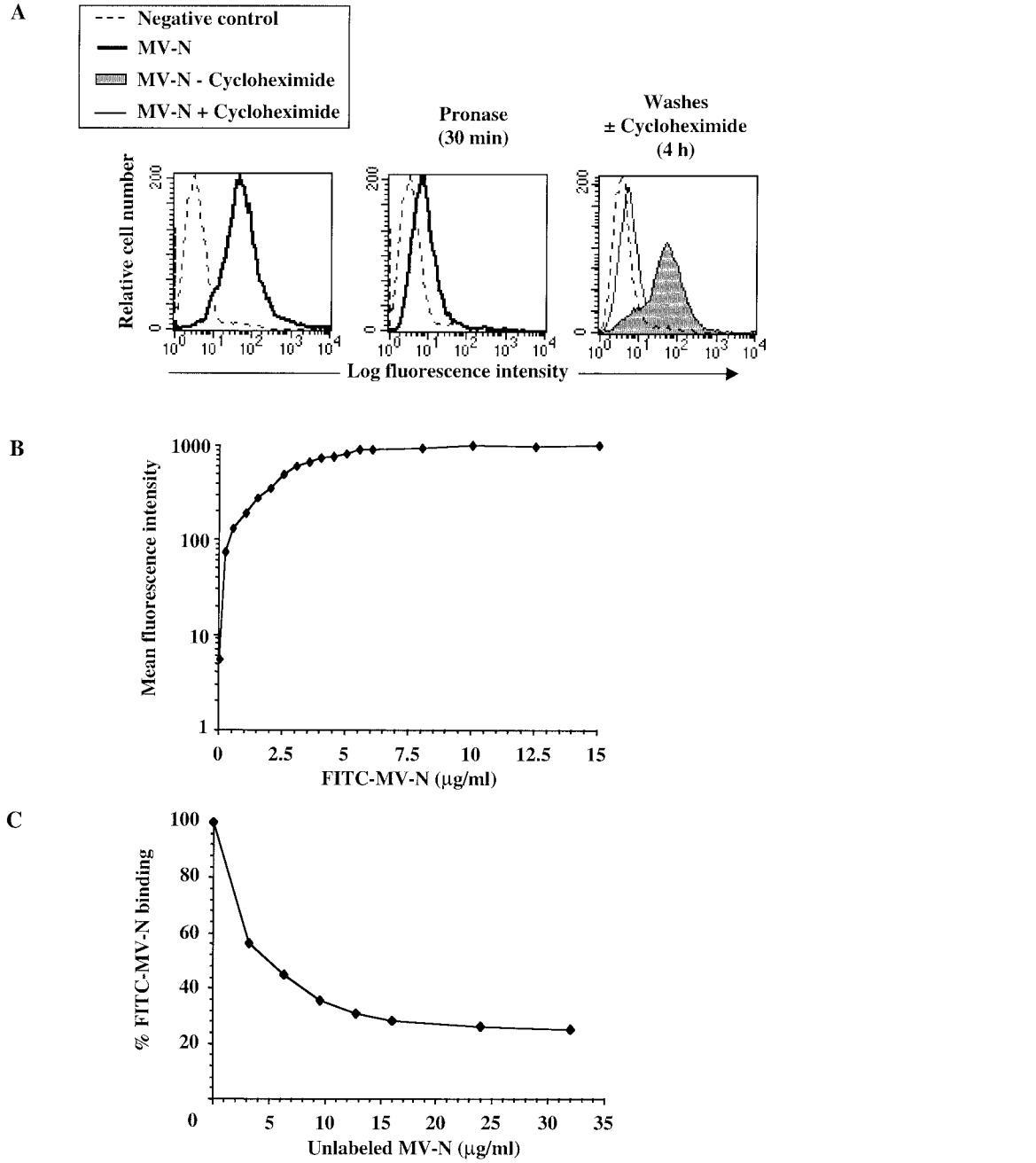

FIG. 3. Specific binding of MV-N to a protein receptor distinct from FcγRII. (A) Requirement of protein synthesis for recovery of MV-N-binding activity after protease treatment. TEC were untreated (left panel) or treated with pronase (middle panel) before MV-N binding. Pronase-treated TEC were incubated for 4 h at 37°C in the absence (gray histogram) or in the presence of cycloheximide (thin line), prior to MV-N binding (right panel). As a negative control, cells were incubated with specific anti-MV-N (Cl25) MAb and streptavidin-PE in the absence of MV-N (dotted line). (B) Dose-dependent binding of FITC-labeled MV-N. TEC were incubated 1 h at 4°C with various amounts of FITC-MV-N, followed by extensive washes prior to flow cytometry analysis. (C) Competition between unlabeled MV-N and FITC-MV-N. Cells were incubated with FITC-MV-N (2.5 μg/well, corresponding to 50% of binding) and increasing amounts of unlabeled MV-N. Percentages of labeled MV-N binding were reported and calculated assuming that the MFI observed with FITC-MV-N alone is 100%. The results are representative from one of three independent experiments.

ing to the cell surface of IIA1.6 Hu FcγRIIb1 (Fig. 2C). Altogether, these results show that MV-N binds both to cells expressing or lacking FcγRII, suggesting the existence of a novel cell surface receptor for MV-N.

MV-N specifically binds to a novel cell surface protein receptor. We next investigated the biochemical characteristics of the MV-N receptor expressed on TEC. Cells were incubated at 37°C for 30 min with pronase prior to MV-N-binding assays.

As shown in Fig. 3A, pronase treatment of TEC resulted in the inhibition of MV-N binding: 90% of untreated cells were competent for MV-N binding (left panel), whereas only 25 to 30% bound MV-N after pronase treatment (middle panel). To analyze the regeneration of MV-N binding, pronase-treated TEC were cultured for 4 h at 37°C in the presence or absence of cycloheximide prior to MV-N binding assays (Fig. 3A, right panel). When pronase-treated TEC were incubated for 4 h in medium alone, up to 80% of MV-N binding was recovered (gray histogram). In contrast, the proportion of MV-N binding remained between 10 to 18% when cycloheximide was added to the medium (thin line). Similar results were obtained with papain or trypsin treatment (data not shown). These results demonstrate that protein synthesis is required for MV-N binding to occur on the cell surface of TEC.

To further demonstrate the specificity of MV-N binding to TEC, we used recombinant MV-N from insect cells labeled with fluorescein (FITC-MV-N). As illustrated in Fig. 3B, FITC-MV-N binding is saturable. Furthermore, competition experiments indicated that a 10-fold excess of unlabeled MV-N is required to inhibit FITC-MV-N binding by 70% (Fig. 3C). Altogether, these results support the conclusion that binding of MV-N to TEC is mediated by a specific protein receptor: the NR.

Both *Morbillivirus*-N and N_{TAIL}, but not N_{CORE}, bind to NR. Since the amino acid sequence of N is well conserved within the *Morbillivirus* genus (10), we hypothesized that PPRV-N, RPV-N, and CDV-N may share common binding properties with MV-N. Like MV-N, purified recombinant PPRV-N and CDV-N bound both to cells expressing or lacking FcγRII (Fig. 4A). Conversely, binding of RPV-N did not involve FcγRII, as indicated by the lack of binding to Hu FcγRIIb1 (Fig. 4A). To exclude the possibility that this binding activity may be due to the self-polymerization property of *Morbillivirus*-N, we used the unrelated NC from RV, a virus belonging to the *Rhabdoviridae* family. Like MV-N, the unrelated NC RV-N possesses the ability to self-assemble to form NC (41). No RV-N binding was detected on TEC expressing NR (data not shown), suggesting that NR is not a receptor for NC structures but binds specifically to *Morbillivirus*-N.

Since the N_{TAIL} domain of *Morbillivirus*-N protrudes from the surface of viral NC (21), we hypothesized that binding of MV-N to NR may be mediated by N_{TAIL}. To test this possibility, we compared the ability of NR to bind to N_{TAIL} and N_{CORE} purified from bacteria. As shown in Fig. 4B (top, left panel), MV-N was partially degraded, as already reported in the case of MV-N purified from virions (15). Limited proteolysis of bacterially purified MV-N in the presence of trypsin resulted in the obtention of a 43-kDa fragment, which corresponds to N_{CORE} (Fig. 4B). No fragment corresponding to the remaining 15 to 17 kDa (N_{TAIL}) was detected, indicating that it is hypersensitive to proteolysis and entirely degraded (25). The bacterially purified N_{TAIL} domain is also shown in Fig. 4B (top, right panel).

Two anti-MV-N MAbs, Cl120 (recognizing aa 133 to 140) and Cl25 (recognizing aa 466 to 474), were used to specifically detect N_{CORE} and N_{TAIL}, respectively (Fig. 4B, bottom). In contrast to MV-N, no binding of N_{CORE} to NR is detected with anti-N Cl120 MAb, even with N_{CORE} amounts as high as 30 μg/well (Fig. 4C, left panel, and data not shown). Using the anti-N Cl25 MAb, but not with anti-N Cl120 MAb, we observed binding of N_{TAIL} to NR (Fig. 4C, right panel, and data not shown). As for MV-N, binding of N_{TAIL} to NR was not blocked by anti-FcγRII MAb (data not shown). In addition, protein synthesis was also required for N_{TAIL}-binding activity on the cell surface of TEC (data not shown). To further demonstrate the specific binding activity of N_{TAIL} to TEC, we performed competition experiments by coincubating 2.5 μg of purified MV-N/well with increasing amounts of N_{TAIL}. As shown in Fig. 4D, N_{TAIL} significantly inhibited the binding of MV-N (55 to 70%) in a dose-dependent manner, whereas N_{CORE} fails to do so. Altogether, these results demonstrate that the region responsible for specific binding to NR is located within the N_{TAIL} domain of MV-N.

Recombinant MV-N is internalized in TEC. We then analyzed the ability of MV-N to bind to the cell surface of TEC after incubation at 37 and 4°C. A strong decrease (20 to 70%) in the amount of MV-N detected on the cell surface was observed as a function of time when TEC were incubated at 37°C, whereas only a slight decrease was observed at 4°C (Fig. 5A, left panel). Similar results were obtained with N_{TAIL} (Fig. 5A, right panel), thus ruling out the possibility that the self-assembled nature of MV-N is responsible for binding to NR. The observed drop in the amount of MV-N on the cell surface suggested that it may be internalized. This hypothesis was confirmed by confocal microscopy analyses (Fig. 5B). MV-N was exclusively present at the plasma membrane level when incubated at 4°C (upper panels). However, no uniform fluorescence was observed, suggesting cell surface MV-N/NR clustering. After 1 h at 37°C, cellular redistribution of MV-N was observed: in particular, through a strong decrease of the fluorescence at the plasma membrane, with the concomitant accumulation in vesicle-like structures within the cytoplasm (lower panels). These results suggest that internalization may occur either by fluid-phase pinocytosis or receptor-mediated endocytosis. MV-N internalization is not toxic for TEC, as indicated by the fact that no apoptosis, as judged by Hoechst staining, was observed after 1 h at both 4 and 37°C (data not shown).

Recombinant MV-N binding to NR on TEC induces cell cycle growth arrest rather than apoptosis. We investigated whether MV-N could affect TEC biology through NR engagement. For this purpose, we studied Ca^{2+} mobilization. A transient intracellular free Ca^{2+} increase in response to the ionophore ionomycin was observed (Fig. 6A). In the presence of MV-N, changes in Ca^{2+} concentration were observed. First, MV-N alone induced a small, but significant, increase in the intracellular free Ca^{2+} basal level. Second, costimulation with ionomycin and MV-N elicited a sustained Ca^{2+} signal.

Since changes in the Ca^{2+} concentration affect the balance between proliferation and differentiation in epithelial cells (5, 6, 37, 56, 65), we therefore examined whether MV-N binding modulates TEC proliferation. As illustrated in Fig. 6B, MV-N, purified from insect cells (not shown) and bacteria, inhibited spontaneous TEC proliferation in a dose-dependent manner (18 to 95%, left panel). Moreover, N_{TAIL} (right panel), but not N_{CORE} (middle panel), also inhibited TEC proliferation by 10 to 95%, indicating that the inhibition of cell proliferation is NC independent.

We next analyzed the cell cycle distribution of MV-N-treated TEC. As illustrated in Fig. 6C, we observed a significant decrease (81% inhibition) in the percentage of MV-N-

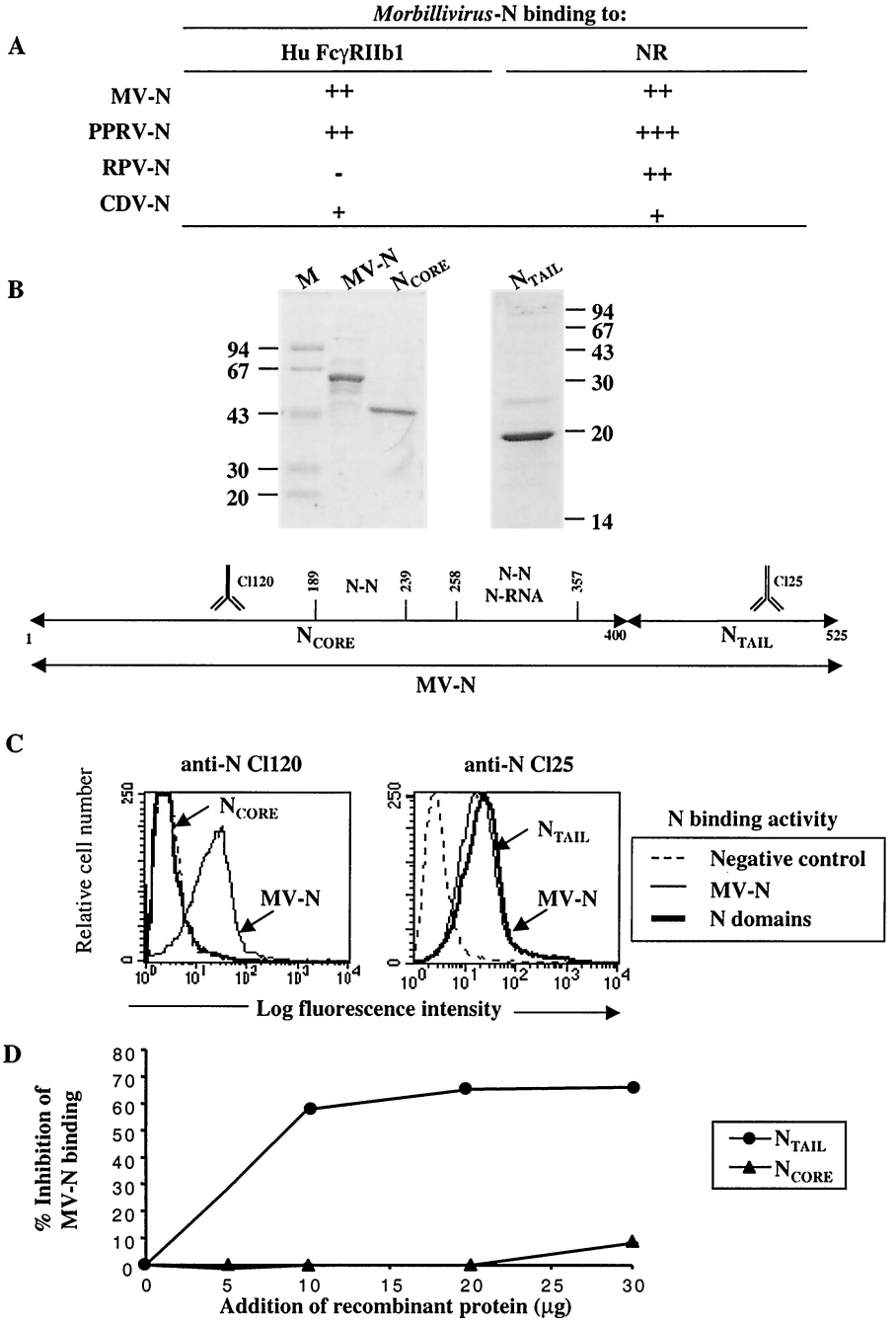

FIG. 4. *Morbillivirus*-N and N_{TAIL} binding to cell surface receptor(s). (A) Binding of *Morbillivirus*-N to different cell lines expressing or not expressing FcγRII. The extent of binding has been evaluated as described in Materials and Methods. The MFI is indicated as follows: −, no binding; +, ++, and +++, MFI values of ca. 10, between 10 and 100, and >100, respectively. The results are representative of three to six independent experiments. (B) At the top of the panel is shown MV-N domain purification from bacteria. Purified proteins were separated by sodium dodecyl sulfate–15% polyacrylamide gel electrophoresis and stained with Coomassie brillant blue. M, molecular mass markers. At the bottom of the panel is shown MV-N domain organization. MV-N (aa 1 to 525) is divided into two domains: N_{CORE} (aa 1 to 400) and N_{TAIL} (aa 401 to 525). The epitopes recognized by the anti-MV-N Cl120 and Cl25 MAbs are indicated. N-N and N-RNA binding sites are also shown. (C) Binding of MV N_{TAIL}, but not N_{CORE}, to NR. TEC were incubated with 5 μg of purified MV-tagged N (thin line) prior to flow cytometry analysis. Binding of N_{CORE} and N_{TAIL} (5 μg, heavy line) was detected by using biotinylated anti-MV-N Cl120 (left panel) and Cl25 (right panel), respectively, and then revealed with streptavidin-PE. As a negative control, neither N nor N domains were added, and the cell lines were incubated in the presence of specific biotinylated anti-N MAb and streptavidin-PE (dotted line). The results are representative from one of three independent experiments. (D) Specific N_{TAIL} binding to NR. Competition binding experiments were performed by incubating MV-N (2.5 μg, corresponding to 50% of binding) with increasing amounts of either N_{TAIL} or N_{CORE}. Bacterially purified MV-N binding was revealed by biotinylated anti-MV-N Cl120 or Cl25 MAbs, depending upon whether N_{TAIL} or N_{CORE} was used as a competitor, respectively. The percentage of MV-N binding inhibition was calculated assuming that the MFI observed with MV-N alone represents 0% of inhibition. The results are representative from one to three independent experiments.

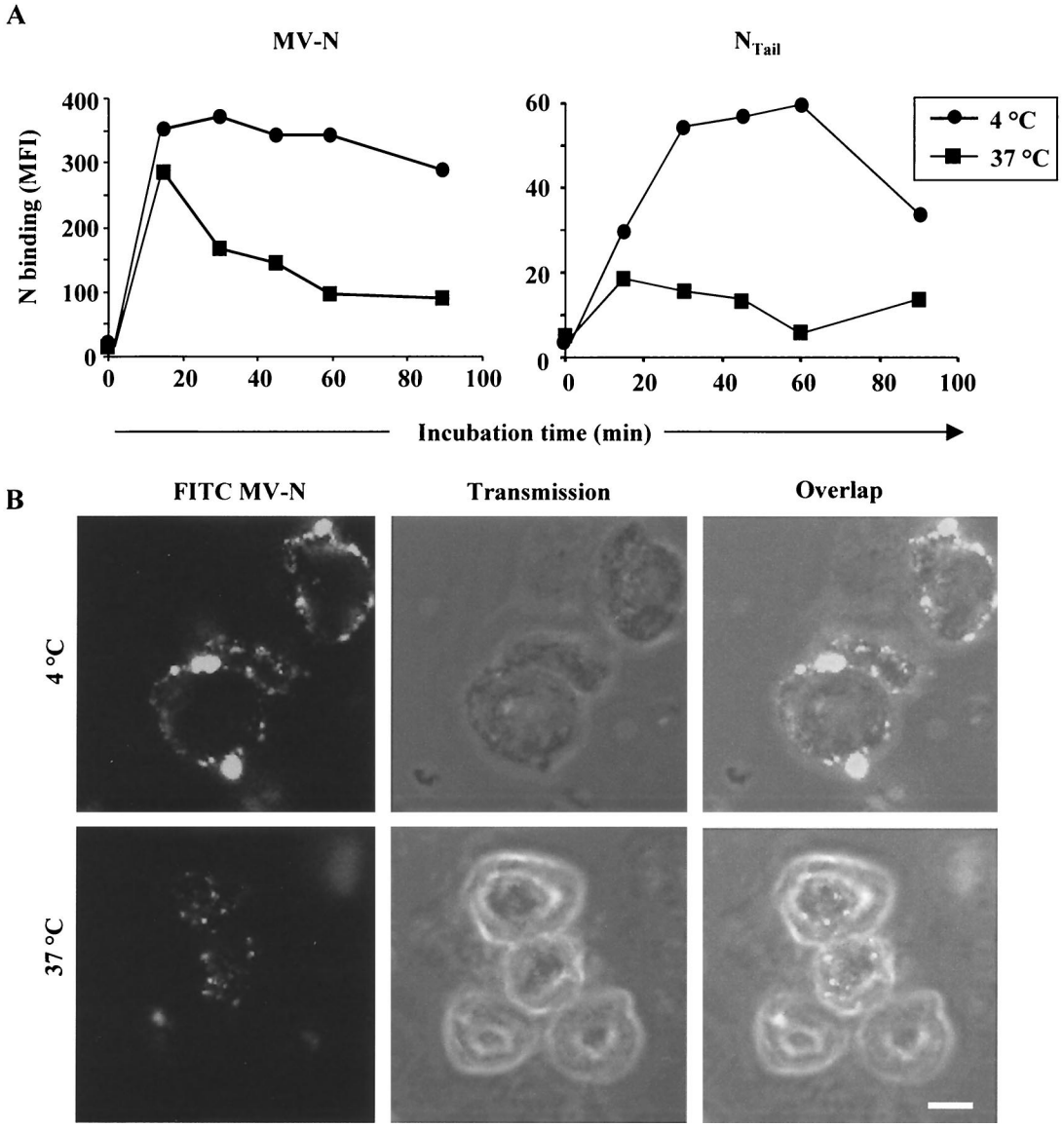

FIG. 5. MV-N constitutive internalization in TEC. (A) Downregulation of MV-N binding in TEC. MV-N binding to TEC was measured at either 4 or 37°C by flow cytometry. Binding of recombinant MV-N (left panel) and N_{TAIL} (right panel) was revealed by using anti-MV-N (Cl25) and streptavidin-PE. The results are representative of three independent experiments (SD values were <15%). (B) MV-N internalization at 37°C in vesicle-like structures within the cytoplasm. FITC-MV-N was used for confocal microscopy analysis. Single confocal sections show FITC fluorescence (left panel), transmission (middle panel), and overlap of both (right panel). Pictures are taken on TEC at either 4°C (upper panel) or 37°C (lower panel) after 1 h of incubation. Shown are representative results from one of three independent experiments. The white scale bar shown in the lower right panel corresponds to 5 μm.

treated TEC in the S phase of the cell cycle by day 2 compared to untreated cells (left panel). Moreover, an accumulation in the G_0/G_1 of the cell cycle (70%) was subsequently observed after MV-N treatment (right panel). Finally, neither MV-N-, N_{TAIL}-, nor N_{CORE}-treated TEC undergo apoptosis, as shown by $DIOC_6$/PI or Hoechst staining (Fig. 6D and data not shown). Altogether, these results demonstrate that MV-N is not toxic but specifically induces a cell cycle arrest rather than apoptosis. Moreover, these results indicate that the N_{TAIL} domain is responsible for these biological effects.

Recombinant MV-N binds to NR on a large number of cell types and species. We then focused on the cellular distribution of putative MV-N receptor(s) different from FcγRII. We used human, murine, and monkey cell lines, as well as freshly isolated human and murine cells (from wild-type [wt] mice or mice lacking FcγRII/III). As illustrated in Table 1, binding of MV-N to human, murine, or monkey epithelial cells and fibroblasts was observed. Moreover, no inhibition of MV-N binding is obtained after treatment with blocking anti-FcγRII/III MAb, indicating that MV-N binds to NR. MV-N binding to human or

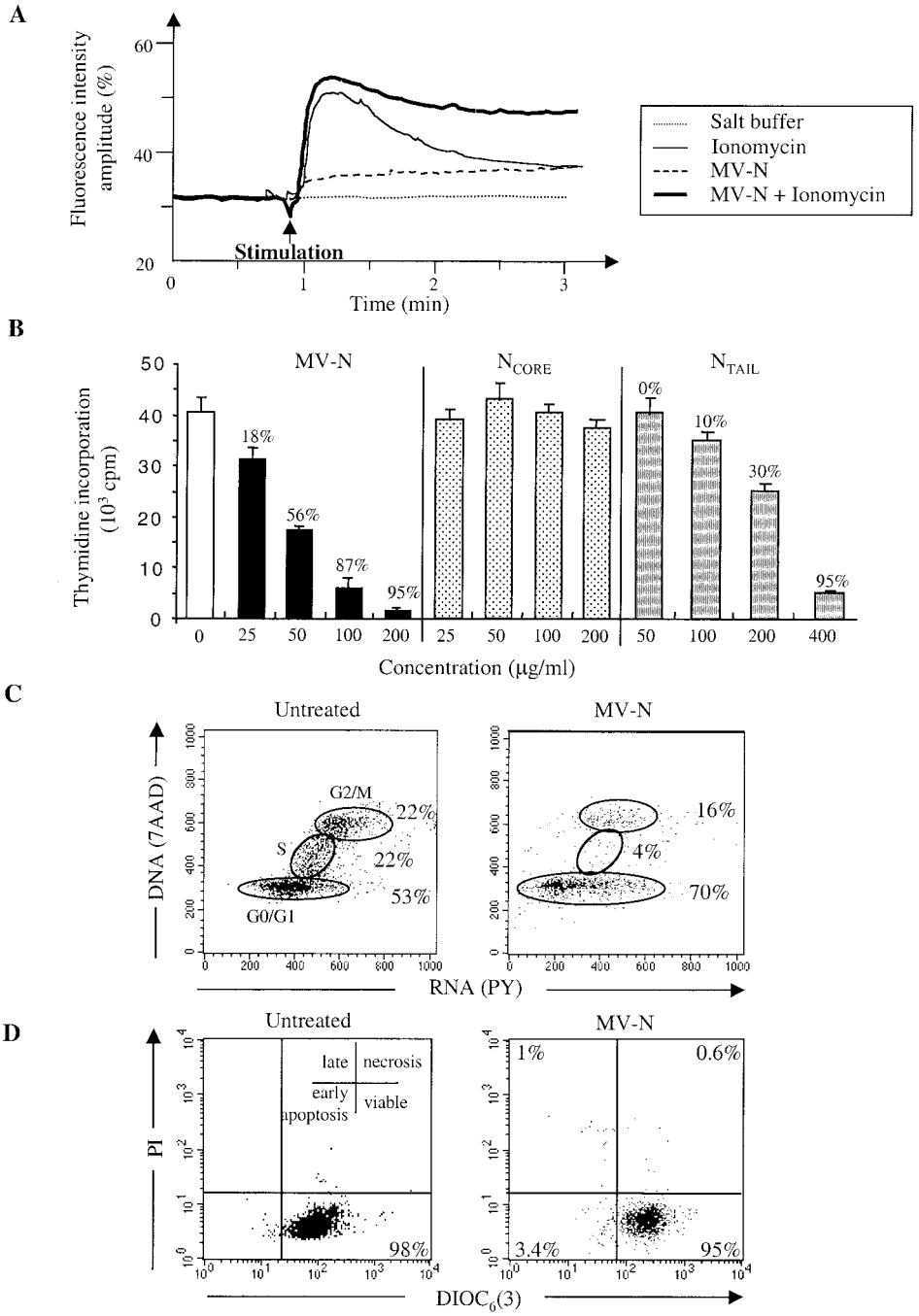

FIG. 6. NR is functional upon MV-N binding. (A) MV-N sustains ionomycin-mediated Ca^{2+} mobilization in TEC. At the time indicated by the arrow, 2 ml of loaded TEC (2×10^5/ml) was stimulated with salt buffer, MV-N (40 μg/ml), and/or ionomycin (10^{-5} M). Cytosolic Ca^{2+} influx was then measured. (B) Effect of MV-N or N_{TAIL} on spontaneous TEC proliferation. TEC were incubated with medium alone (open bar, control) and with various amounts of bacterially purified recombinant MV-N (solid bars), N_{CORE} (dotted bars), or N_{TAIL} (gray bars). Each value represents mean ± the SD of triplicate cultures. (C) Cell cycle analysis of TEC with 7AAD(DNA)/PY(RNA) staining. Two-dimensional analysis of DNA/RNA content is shown. The percentages of cells in the G_0/G_1, S, and G_2/M phases of the cell cycle are shown. TEC were untreated or treated for 2 days with 200 μg of MV-N/ml purified from insect cells. (D) Viability and apoptosis were analyzed by flow cytometry in untreated TEC and in MV-N-treated TEC as in panel C after $DIOC_6$/PI double staining. Viable cells are $DIOC_6$ positive and PI negative. In contrast, apoptotic cells have both a decrease of mitochondrial transmembrane potential and permeabilized membranes that render them $DIOC_6$ negative and PI positive, respectively. The results are from one representative experiment out of three.

wt murine monocytes, DC, and B cells was also observed. This binding activity was partially inhibited by anti-FcγRII/III MAb, suggesting that the binding of MV-N relies partly on FcγRII/III (Table 1). Binding of MV-N to NR on these cells was confirmed in FcγRII/III$^{-/-}$ mice (Table 1). N_{TAIL} also bound to human NR on lymphoid and nonlymphoid cell surface (data not shown). Although no MV-N-binding activity was detected on red blood cells and both human and murine resting T cells,

TABLE 1. MV-N binding on different cell types

Cell type[a]	N binding (MFI)[b]	Inhibition of N binding by anti-FcγRII ± III[c]	FcγRII expression[d]	Predictive NR expression[e]
Epithelial cell lines				
P1.4D6 (human postnatal cortical TEC)	++	No	−	+
3D1 (mouse cortical TEC)	+	No	−	+
HeLa (human carcinoma)	+	No	−	+
Fibroblast cell lines				
MeWo (human melanoma)	+	No	−	+
NIH 3T3 (mouse)	++	No	−	+
Vero (monkey)	+	ND[f]	−	+
Monocytes/macrophages				
Human	+	Partial	+	+
Mouse wt	+++	Partial	+	+
Mouse FcγRII/III$^{-/-}$	++	No	−	+
DC				
Human	+	Partial	+	+
Mouse wt	+++	Partial	+	+
Mouse FcγRII/III$^{-/-}$	++	No	−	+
B cells				
Primary resting mouse wt	+++	Partial	+	+
Primary resting mouse FcγRII/III$^{-/-}$	++	No	−	+
T cells				
Primary resting human	−	No	−	−
Primary resting mouse wt	−	No	−	−
Primary resting mouse FcγRII/III$^{-/-}$	−	No	−	−
Human Jurkat	+	No	−	+
Human red blood cells	−	No	−	−

[a] Human and murine cells were isolated as described in Materials and Methods.
[b] MV-N binding was performed as described in Fig. 2. However, MV-N binding to murine primary cells was assessed by double stainings. The results are expressed as described in Materials and Methods. MFI is indicated as follows: −, no binding; +, MFI between 10 and 50; ++, MFI between 50 and 100; +++, MFI >100.
[c] Inhibition of MV-N binding was determined after incubation of MV-N with blocking KB61 or 2.4G2 MAb against human or murine FcγRII/III, respectively. The results are expressed as the inhibition percentage of MFI and are indicated as no inhibition (no) or 30 to 70% inhibition (partial).
[d] FcγRII/III expression was determined by using anti-human and anti-murine CD32/CD16 MAbs and is indicated as no expression (−) or FcγRII ± III expression (+).
[e] Putative second receptor expression was deduced by analysis of MV-N bindings. All labelings were analyzed by flow cytometry, and data are expressed as the mean of three to five separate experiments (SD values are <15%).
[f] ND, not determined.

MV-N binds to a human Jurkat T-cell line independently of FcγRII expression (Table 1), suggesting that MV-N binds to NR on human activated T cells.

Upon binding to NR on human activated T cells, MV-N inhibits cell proliferation. To further demonstrate that NR is induced after T-cell activation, human T cells were freshly purified from the peripheral blood and then activated with phorbol myristate acetate plus ionomycin for 16 h. After extensive washes, MV-N was added, and activated T cells were assayed for FcR expression and MV-N-binding ability at different time intervals. Although no significant FcγRII expression was detected on the activated T-cell surface (Fig. 7A), MV-N binding was observed by as early as day 1 (Fig. 7B). This binding activity reached a maximum on day 2 and then slowly decreased on day 3, indicating that NR is readily induced after T-cell activation. Finally, we examined whether MV-N binding modulates T-cell proliferation. As shown in Fig. 7C, MV-N inhibited mitogen-induced T-cell proliferation in a dose-dependent manner. Finally, no apoptosis was observed under these conditions (data not shown), indicating that MV-N induces suppression of T-cell proliferation rather than apoptosis.

DISCUSSION

Combined mechanisms account for MV-induced immunosuppression (see reviews, references 38, 51, and 53). Among them, inhibition of cell proliferation of both MV-infected and uninfected cells has been reported. The latter activity suggested a role of MV proteins in such events. Thus far, H and F glycoproteins expressed at the surface of MV-infected cell, as well as binding of recombinant MV-N protein from insect cells to human and murine FcγRII, have been reported to suppress immune responses of uninfected cells (34, 45, 49). Although MV-N is considered as an internal protein located either in MV-infected cells or inside the virion, humoral responses against N suggest that N is exposed on the cell surface in the course of MV infection. The results reported here provide the first experimental evidence for the release of MV-N in the extracellular compartment, where it becomes accessible to a novel cell surface receptor possibly involved in MV-induced immunosuppression.

The present study shows release of N in the extracellular compartment after apoptosis and/or secondary necrosis of

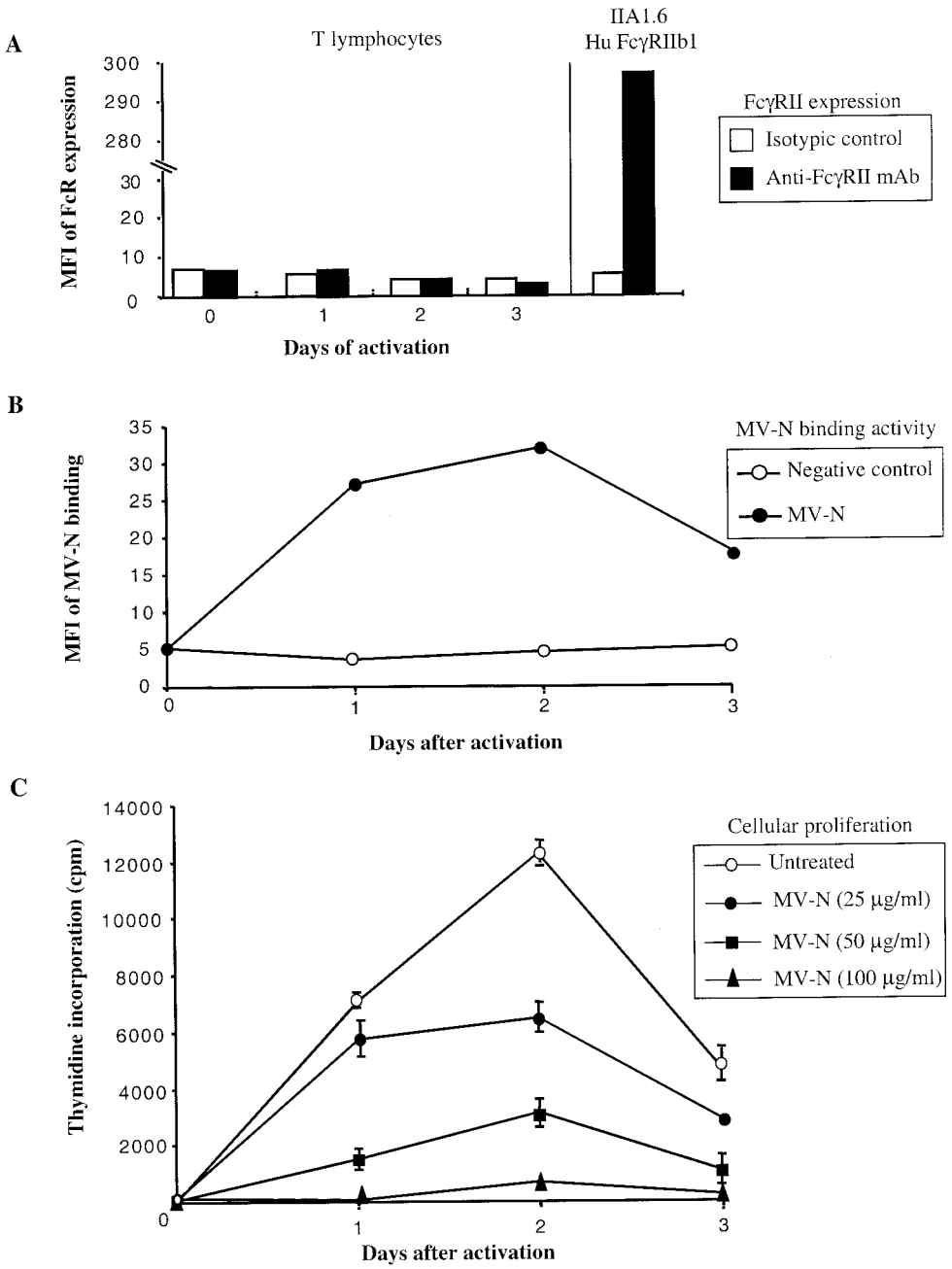

FIG. 7. Inhibition of human activated T-cell proliferation after MV-N binding to NR. (A) FcγRII expression on human activated T cells was detected by using anti-CD32-PE at different times after stimulation. (B) MV-N binding was detected with specific biotinylated anti-MV-N (Cl25) and then revealed with streptavidin-PE prior to flow cytometry analysis. Cells were incubated with 5 μg of purified recombinant MV-N from insect cells (●). As a negative control, cells were incubated without MV-N in the presence of anti-MV-N (Cl25) and streptavidin-PE (○). The experiments were performed twice, and the SD values were <10%. (C) Effect of MV-N on human activated T-cell proliferation. Activated T cells were incubated with either medium alone (○) or with various amounts of recombinant MV-N from insect cells (●, ■, and ▲) for 24, 48, or 72 h. Each value represents the mean ± SD of triplicate cultures. The results are from one representative experiment out of three.

MV-infected human TEC. MV initially replicates in the respiratory tracts and then spreads to the local lymphoid tissue. This second viremia allows the spreading of the virus to other lymphoid organs, including the thymus, where a profound thymic injury, characterized by degenerative and/or necrotic lesions, occurs (8, 62). Human thymic stromal cells, particularly TEC, have been described as targets for MV during the acute phase of infection (35, 64). In a SCID-hu thymic implant model, MV infection of TEC cause apoptosis of uninfected thymocytes (1). These observations might be ascribed to apoptosis of TEC replicating MV in vitro (58). Interestingly, our findings clearly indicate that both MV replication and apoptosis of MV-infected TEC are required for extracellular release of high amounts of N. These observations are consistent with the fact

that MV-N is the major constituent of cytosolic MV proteins in infected cells and suggest that sufficient amounts of extracellular N are present in the thymus to be accessible to cell surface receptors. In agreement with this hypothesis, our results indicate that MV-N is detected on the cell surface of living MV-infected TEC. This suggests that N, once released in the extracellular compartment, is capable of interacting with cell surface receptor(s) on neighboring MV-infected and uninfected cells, affecting their biology.

Here, we report that viral and recombinant MV-N specifically interacts with a novel cell surface protein receptor on TEC, different from FcγRII, that we call NR. Genetic and biochemical studies of *Morbillivirus*-N have revealed that the hydrophobic N-terminal domain (N_{CORE}) is involved in RNA binding and NC assembly, whereas the flexible C-terminal domain (N_{TAIL}) is involved in binding to P (2, 7, 9, 25, 31, 32). For several reasons, we excluded that RNA and/or the self-assembled state of MV-N could be involved in binding of N to NR. MV-N binding to NR is specific and is not simply due to an interaction of NC at the cell surface, as indicated by the fact that the nonrelated NC from RV-N is not able to bind to NR. In addition, we show that bacterially expressed N_{TAIL}, which contains no RNA and has no self-assembling properties (32), is necessary and sufficient for binding to NR. Conversely, the N_{CORE} domain, which still forms NC-like structures (32), does not bind to NR and does not inhibit MV-N binding. Therefore, our results rule out the possibility that MV-N binding to NR can be mediated by N-associated RNA or by NC-like particles. Experimental evidence indicates that the N_{TAIL} domain of MV-N is accessible on the surface of NC-like structures (21). Moreover, recent data indicate that N_{TAIL} is an intrinsically unstructured monomer in solution (32). The presence of flexible regions exposed at the surface of the viral NC would ideally favor the interaction with different viral and cellular partners, including NR.

Constitutive expression of NR is not restricted to TEC, since it is also detected on lymphoid and nonlymphoid cells from human, monkey, and mouse sources. Even if we cannot conclude whether MV-N binds to the same receptor on these different cell types, one can speculate that NR might be ubiquitous and conserved among different species. According to this hypothesis, we found that four *Morbillivirus*-N proteins bind to receptors exposed at the cell surface of different cell lines from different species, which do not correspond to their natural hosts. Indeed, PPRV-N and CDV-N bind to both human FcγRIIs and human and murine NR, whereas RPV-N only binds to NR. These results suggest that most *Morbillivirus*-N proteins share conserved FcγRII and NR on their respective hosts and that these receptors may derive from a common ancestral receptor. In agreement with this hypothesis, mammalian FcγRIIs are conserved among species (22).

Notably, our data clearly indicate that MV-N/NR engagement on TEC leads to signal transduction by modulating Ca^{2+} influx and to the inhibition of spontaneous cell proliferation by inducing an arrest in the G_0/G_1 phases of the cell cycle. We also show that MV-N or N_{TAIL} binding to uninfected TEC induces growth arrest independently of apoptosis. Growth arrest has also been noted upon interaction of MV-H and-F proteins with uninfected cells (20, 49, 52), strongly suggesting that MV viral proteins share the ability to inhibit cell proliferation through unidentified cellular receptors. MV replication is responsible for thymic involution (8, 62). However, thymic epithelium disruption could also be responsible for extracellular release of N after apoptosis of MV-infected TEC. Once in the extracellular compartment, MV-N can bind to NR on neighboring uninfected TEC and inhibits their proliferation. This activity accounts for thymocyte survival signal privation. This default in survival signal could cause immature thymocyte apoptosis, as previously observed (1). However, recent reports indicate that during the acute phase of MV infection no decrease thymic output is observed, suggesting that thymic atrophy is not responsible for lymphopenia (40). Homeostatic regulation processes could occur to compensate immature thymocyte apoptosis, through an as-yet-unidentified mechanism, resulting in an increase in the impaired functional T-lymphocyte output (40, 47). Finally, our data indicate that NR is induced after human T-cell activation and that binding of MV-N to NR inhibits their proliferation. Immunosuppression is established in the presence of limited number of infected peripheral blood cells, suggesting that indirect events occur. Virus-induced apoptosis, modulation of cytokine production, and interaction of MV-H/F with uninfected T cells have been postulated to disrupt T-cell-mediated immune responses (26, 49, 53). Here, we describe a novel mechanism whereby the release of N from neighboring apoptotic MV-infected cells suppresses activated T-cell proliferation through NR engagement in tissues.

By showing that N is released in the extracellular compartment after apoptosis of MV-infected cells, we provide evidences that MV-N binding to extracellular receptors is responsible for the nucleoprotein dual functions. The biochemical characterization of NR is expected to provide new insights into the mechanisms underlying *Morbillivirus* pathogenesis.

ACKNOWLEDGMENTS

We thank K. Ravanel, V. Lotteau, P. André, D. Kaizerlian, B. Horvat, C. Servet-Delprat, and M. Amélie-Moradies for scientific advice during this study. We also thank Y. Zaffran and A. Astier for critical review of the manuscript. We particularly thank M. A. Billeter for providing the recombinant and chimeric MV. We are grateful to C. Roche and J. Abello for providing the fluorimeter to analyze calcium influx. The expert technical assistance of F. Duchamp, P. Galia, C. Bella, M. Flacher, and M. Rossi is also acknowledged. We thank C. Kai for providing the anti-CDV-N MAbs. We also thank R. Buckland and M. Lafon for providing the plasmids coding for CDV-N and RV-N, respectively.

This work was supported in part by institutional grants from the Ministère de l'Education Nationale, de l'Enseignement Supérieur, et de la Recherche and from the Institut National de la Santé et de la Recherche Médicale and by additional support from the Association pour la Recherche sur le Cancer (CRC 5753) and the Programme de Recherche de la Région Rhône-Alpes (UR503-2A7-HHC02F). J. C. Marie was supported by the Human Frontier Science Program.

REFERENCES

1. **Auwaerter, P. G., H. Kaneshima, J. M. McCune, G. Wiegand, and D. E. Griffin.** 1996. Measles virus infection of thymic epithelium in the SCID-hu mouse leads to thymocyte apoptosis. J. Virol. **70:**3734–3740.
2. **Bankamp, B., S. M. Horikami, P. D. Thompson, M. Huber, M. Billeter, and S. A. Moyer.** 1996. Domains of the measles virus N protein required for binding to P protein and self-assembly. Virology **216:**272–277.
3. **Barrett, T.** 1999. Morbillivirus infections, with special emphasis on morbilliviruses of carnivores. Vet. Microbiol. **69:**3–13.
4. **Bhella, D., A. Ralph, L. B. Murphy, and R. P. Yeo.** 2002. Significant differences in nucleocapsid morphology within the *Paramyxoviridae*. J. Gen. Virol. **83:**1831–1839.

5. **Bikle, D. D., A. Ratnam, T. Mauro, J. Harris, and S. Pillai.** 1996. Changes in calcium responsiveness and handling during keratinocyte differentiation: potential role of the calcium receptor. J. Clin. Investig. **97:**1085–1093.
6. **Black, B. L., and J. E. Smith.** 1989. Regulation of goblet cell differentiation by calcium in embryonic chick intestine. FASEB J. **3:**2653–2659.
7. **Buchholz, C. J., D. Spehner, R. Drillien, W. J. Neubert, and H. E. Homann.** 1993. The conserved N-terminal region of Sendai virus nucleocapsid protein NP is required for nucleocapsid assembly. J. Virol. **67:**5803–5812.
8. **Chino, F., H. Kodama, T. Ohkawa, and Y. Egashira.** 1979. Alterations of the thymus and peripheral lymphoid tissues in fatal measles: a review of 14 autopsy cases. Acta Pathol. Jpn. **29:**493–507.
9. **Curran, J., H. Homann, C. Buchholz, S. Rochat, W. Neubert, and D. Kolakofsky.** 1993. The hypervariable C-terminal tail of the Sendai paramyxovirus nucleocapsid protein is required for template function but not for RNA encapsidation. J. Virol. **67:**4358–4364.
10. **Diallo, A., T. Barrett, M. Barbron, G. Meyer, and P. C. Lefevre.** 1994. Cloning of the nucleocapsid protein gene of peste-des-petits-ruminants virus: relationship to other morbilliviruses. J. Gen. Virol. **75:**233–237.
11. **Escoffier, C., S. Manie, S. Vincent, C. P. Muller, M. Billeter, and D. Gerlier.** 1999. Nonstructural C protein is required for efficient measles virus replication in human peripheral blood cells. J. Virol. **73:**1695–1698.
12. **Etchart, N., P. O. Desmoulins, K. Chemin, C. Maliszewski, B. Dubois, F. Wild, and D. Kaiserlian.** 2001. Dendritic cells recruitment and in vivo priming of $CD8^+$ CTL induced by a single topical or transepithelial immunization via the buccal mucosa with measles virus nucleoprotein. J. Immunol. **167:** 384–3891.
13. **Fernandez, E., A. Vicente, A. Zapata, B. Brera, J. J. Lozano, C. Martinez, and M. L. Toribio.** 1994. Establishment and characterization of cloned human thymic epithelial cell lines: analysis of adhesion molecule expression and cytokine production. Blood **83:**3245–3254.
14. **Fugier-Vivier, I., C. Servet-Delprat, P. Rivailler, M. C. Rissoan, Y. J. Liu, and C. Rabourdin-Combe.** 1997. Measles virus suppresses cell-mediated immunity by interfering with survival and functions of dendritic and T cells. J. Exp. Med. **186:**813–823.
15. **Giraudon, P., M. F. Jacquier, and T. F. Wild.** 1988. Antigenic analysis of African measles virus field isolates: identification and localisation of one conserved and two variable epitope sites on the NP protein. Virus Res. **10:**137–152.
16. **Giraudon, P., and T. F. Wild.** 1981. Monoclonal antibodies against measles virus. J. Gen. Virol. **54:**325–332.
17. **Graves, M., D. E. Griffin, R. T. Johnson, R. L. Hirsch, I. L. de Soriano, S. Roedenbeck, and A. Vaisberg.** 1984. Development of antibody to measles virus polypeptides during complicated and uncomplicated measles virus infections. J. Virol. **49:**409–412.
18. **Griffin, D. E.** 1995. Immune responses during measles virus infection. Curr. Top. Microbiol. Immunol. **191:**117–134.
19. **Harty, R. N., and P. Palese.** 1995. Measles virus phosphoprotein (P) requires the NH2- and COOH-terminal domains for interactions with the nucleoprotein (N) but only the COOH terminus for interactions with itself. J. Gen. Virol. **76:**2863–2867.
20. **Heaney, J., T. Barrett, and S. L. Cosby.** 2002. Inhibition of in vitro leukocyte proliferation by morbilliviruses. J. Virol. **76:**3579–3584.
21. **Heggeness, M. H., A. Scheid, and P. W. Choppin.** 1980. Conformation of the helical nucleocapsids of paramyxoviruses and vesicular stomatitis virus: reversible coiling and uncoiling induced by changes in salt concentration. Proc. Natl. Acad. Sci. USA **77:**2631–2635.
22. **Hughes, A. L.** 1996. Gene duplication and recombination in the evolution of mammalian Fc receptors. J. Mol. Evol. **43:**4–10.
23. **Ilonen, J., M. J. Makela, B. Ziola, and A. A. Salmi.** 1990. Cloning of human T cells specific for measles virus haemagglutinin and nucleocapsid. Clin. Exp. Immunol. **81:**212–217.
24. **Jacobson, S., R. P. Sekaly, C. L. Jacobson, H. F. McFarland, and E. O. Long.** 1989. HLA class II-restricted presentation of cytoplasmic measles virus antigens to cytotoxic T cells. J. Virol. **63:**1756–1762.
25. **Karlin, D., S. Longhi, and B. Canard.** 2002. Substitution of two residues in the measles virus nucleoprotein results in an impaired self-association. Virology **302:**420–432.
26. **Karp, C. L., M. Wysocka, L. M. Wahl, J. M. Ahearn, P. J. Cuomo, B. Sherry, G. Trinchieri, and D. E. Griffin.** 1996. Mechanism of suppression of cell-mediated immunity by measles virus. Science **273:**228–231.
27. **Kauffman, C. A., A. G. Bergman, and R. P. O'Connor.** 1982. Distemper virus infection in ferrets: an animal model of measles-induced immunosuppression. Clin. Exp. Immunol. **47:**617–625.
28. **Libeau, G., A. Diallo, F. Colas, and L. Guerre.** 1994. Rapid differential diagnosis of rinderpest and peste des petits ruminants using an immunocapture ELISA. Vet. Rec. **134:**300–314.
29. **Libeau, G., and M. Lafon.** 1984. Production of monoclonal antibodies against the Pasteur (P.V.) strain of rabies virus: problems and results. Dev. Biol. Stand. **57:**213–218.
30. **Libeau, G., C. Prehaud, R. Lancelot, F. Colas, L. Guerre, D. H. Bishop, and A. Diallo.** 1995. Development of a competitive ELISA for detecting antibodies to the peste des petits ruminants virus using a recombinant nucleoprotein. Res. Vet. Sci. **58:**50–65.
31. **Liston, P., R. Batal, C. DiFlumeri, and D. J. Briedis.** 1997. Protein interaction domains of the measles virus nucleocapsid protein (NP). Arch. Virol. **142:**305–321.
32. **Longhi, S., V. Receveur-Brechot, D. Karlin, K. Johansson, H. Darbon, D. Bhella, R. Yeo, S. Finet, and B. Canard.** 2003. The C-terminal domain of the measles virus nucleoprotein is intrinsically disordered and folds upon binding to the C-terminal moiety of the phosphoprotein. J. Biol. Chem. **278:** 18638–18648.
33. **Macatonia, S. E., C. S. Hsieh, K. M. Murphy, and A. O'Garra.** 1993. Dendritic cells and macrophages are required for Th1 development of $CD4^+$ T cells from alpha beta TCR transgenic mice: IL-12 substitution for macrophages to stimulate IFN-γ production is IFN-γ-dependent. Int. Immunol. **5:**1119–1128.
34. **Marie, J. C., J. Kehren, M. C. Trescol-Biemont, A. Evlashev, H. Valentin, T. Walzer, R. Tedone, B. Loveland, J. F. Nicolas, C. Rabourdin-Combe, and B. Horvat.** 2001. Mechanism of measles virus-induced suppression of inflammatory immune responses. Immunity. **14:**69–79.
35. **Moench, T. R., D. E. Griffin, C. R. Obriecht, A. J. Vaisberg, and R. T. Johnson.** 1988. Acute measles in patients with and without neurological involvement: distribution of measles virus antigen and RNA. J. Infect. Dis. **158:**433–442.
36. **Norrby, E., and Y. Gollmar.** 1972. Appearance and persistence of antibodies against different virus components after regular measles infections. Infect. Immun. **6:**240–247.
37. **Ochieng, J., Q. S. Tahin, C. C. Booth, and J. Russo.** 1991. Buffering of intracellular calcium in response to increased extracellular levels in mortal, immortal, and transformed human breast epithelial cells. J. Cell. Biochem. **46:**250–254.
38. **Okada, H., T. A. Sato, A. Katayama, K. Higuchi, K. Shichijo, T. Tsuchiya, N. Takayama, Y. Takeuchi, T. Abe, N. Okabe, and M. Tashiro.** 2001. Comparative analysis of host responses related to immunosuppression between measles patients and vaccine recipients with live attenuated measles vaccines. Arch. Virol. **146:**859–874.
39. **Olszewska, W., J. Erume, J. Ripley, M. W. Steward, and C. D. Partidos.** 2001. Immune responses and protection induced by mucosal and systemic immunization with recombinant measles nucleoprotein in a mouse model of measles virus-induced encephalitis. Arch. Virol. **146:**293–302.
40. **Permar, S. R., W. J. Moss, J. J. Ryon, D. C. Douek, M. Monze, and D. E. Griffin.** 2003. Increased thymic output during acute measles virus infection. J. Virol. **77:**7872–7879.
41. **Prehaud, C., R. D. Harris, V. Fulop, C. L. Koh, J. Wong, A. Flamand, and D. H. Bishop.** 1990. Expression, characterization, and purification of a phosphorylated rabies nucleoprotein synthesized in insect cells by baculovirus vectors. Virology **178:**486–497.
42. **Pulford, K., E. Ralfkiaer, S. M. MacDonald, W. N. Erber, B. Falini, K. C. Gatter, and D. Y. Mason.** 1986. A new monoclonal antibody (KB61) recognizing a novel antigen which is selectively expressed on a subpopulation of human B lymphocytes. Immunology **57:**71–76.
43. **Radecke, F., and M. A. Billeter.** 1996. The nonstructural C protein is not essential for multiplication of Edmonston B strain measles virus in cultured cells. Virology **217:**418–421.
44. **Radecke, F., P. Spielhofer, H. Schneider, K. Kaelin, M. Huber, C. Dotsch, G. Christiansen, and M. A. Billeter.** 1995. Rescue of measles viruses from cloned DNA. EMBO J. **14:**5773–5784.
45. **Ravanel, K., C. Castelle, T. Defrance, T. F. Wild, D. Charron, V. Lotteau, and C. Rabourdin-Combe.** 1997. Measles virus nucleocapsid protein binds to FcγRII and inhibits human B-cell antibody production. J. Exp. Med. **186:** 269–278.
46. **Richardson, C. D., A. Scheid, and P. W. Choppin.** 1980. Specific inhibition of paramyxovirus and myxovirus replication by oligopeptides with amino acid sequences similar to those at the N-termini of the F1 or HA2 viral polypeptides. Virology **105:**205–222.
47. **Ryon, J. J., W. J. Moss, M. Monze, and D. E. Griffin.** 2002. Functional and phenotypic changes in circulating lymphocytes from hospitalized zambian children with measles. Clin. Diagn. Lab. Immunol. **9:**994–1003.
48. **Saurin, J. C., E. Nemoz-Gaillard, B. Sordat, J. C. Cuber, D. H. Coy, J. Abello, and J. A. Chayvialle.** 1999. Bombesin stimulates adhesion, spreading, lamellipodia formation, and proliferation in the human colon carcinoma Isreco1 cell line. Cancer Res. **59:**962–967.
49. **Schlender, J., J. J. Schnorr, P. Spielhoffer, T. Cathomen, R. Cattaneo, M. A. Billeter, V. ter Meulen, and S. Schneider-Schaulies.** 1996. Interaction of measles virus glycoproteins with the surface of uninfected peripheral blood lymphocytes induces immunosuppression in vitro. Proc. Natl. Acad. Sci. USA **93:**13194–13199.
50. **Schneider, H., K. Kaelin, and M. A. Billeter.** 1997. Recombinant measles viruses defective for RNA editing and V protein synthesis are viable in cultured cells. Virology **227:**314–322.
51. **Schneider-Schaulies, S., K. Bieback, E. Avota, I. Klagge, and V. ter Meulen.** 2002. Regulation of gene expression in lymphocytes and antigen-presenting

cells by measles virus: consequences for immunomodulation. J. Mol. Med. **80:**73–85.
52. **Schnorr, J. J., M. Seufert, J. Schlender, J. Borst, I. C. Johnston, V. ter Meulen, and S. Schneider-Schaulies.** 1997. Cell cycle arrest rather than apoptosis is associated with measles virus contact-mediated immunosuppression in vitro. J. Gen. Virol. **78:**3217–3226.
53. **Servet-Delprat, C., P.-O. Vidalain, H. Valentin, and C. Rabourdin-Combe.** 2003. Measles virus and dendritic cell functions: how specific response cohabits with immunosuppression. Curr. Top. Microbiol. Immunol. **276:**103–123.
54. **ten Oever, B. R., M. J. Servant, N. Grandvaux, R. Lin, and J. Hiscott.** 2002. Recognition of the measles virus nucleocapsid as a mechanism of IRF-3 activation. J. Virol. **76:**3659–3669.
55. **Toba, K., E. F. Winton, T. Koike, and A. Shibata.** 1995. Simultaneous three-color analysis of the surface phenotype and DNA-RNA quantitation using 7-amino-actinomycin D and pyronin Y. J. Immunol. Methods **182:**193–207.
56. **Tu, C. L., W. Chang, and D. D. Bikle.** 2001. The extracellular calcium-sensing receptor is required for calcium-induced differentiation in human keratinocytes. J. Biol. Chem. **276:**41079–41085.
57. **Unkeless, J. C.** 1979. Characterization of a monoclonal antibody directed against mouse macrophage and lymphocyte Fc receptors. J. Exp. Med. **150:** 580–596.
58. **Valentin, H., O. Azocar, B. Horvat, R. Williems, R. Garrone, A. Evlashev, M. L. Toribio, and C. Rabourdin-Combe.** 1999. Measles virus infection induces terminal differentiation of human thymic epithelial cells. J. Virol. **73:**2212–2221.
59. **van Binnendijk, R. S., M. C. Poelen, P. de Vries, H. O. Voorma, A. D. Osterhaus, and F. G. Uytdehaag.** 1989. Measles virus-specific human T-cell clones: characterization of specificity and function of $CD4^+$ helper/cytotoxic and $CD8^+$ cytotoxic T-cell clones. J. Immunol. **142:**2847–2854.
60. **Van Den Herik-Oudijk, I. E., N. A. Westerdaal, N. V. Henriquez, P. J. Capel, and J. G. Van De Winkel.** 1994. Functional analysis of human Fc gamma RII (CD32) isoforms expressed in B lymphocytes. J. Immunol. **152:**574–585.
61. **Vidalain, P. O., D. Laine, Y. Zaffran, O. Azocar, C. Servet-Delprat, T. F. Wild, C. Rabourdin-Combe, and H. Valentin.** 2002. Interferons mediate terminal differentiation of human cortical thymic epithelial cells. J. Virol. **76:**6415–6424.
62. **White, R. G., and J. F. Boyd.** 1973. The effect of measles on the thymus and other lymphoid tissues. Clin. Exp. Immunol. **13:**343–357.
63. **Wohlsein, P., H. M. Wamwayi, G. Trautwein, J. Pohlenz, B. Liess, and T. Barrett.** 1995. Pathomorphological and immunohistological findings in cattle experimentally infected with rinderpest virus isolates of different pathogenicity. Vet. Microbiol. **44:**141–149.
64. **Yamanouchi, K., F. Chino, F. Kobune, H. Kodama, and T. Tsuruhara.** 1973. Growth of measles virus in the lymphoid tissues of monkeys. J. Infect. Dis. **128:**795–799.
65. **Yuspa, S. H., A. E. Kilkenny, P. M. Steinert, and D. R. Roop.** 1989. Expression of murine epidermal differentiation markers is tightly regulated by restricted extracellular calcium concentrations in vitro. J. Cell Biol. **109:** 1207–1217.
66. **Zhang, X., C. Glendening, H. Linke, C. L. Parks, C. Brooks, S. A. Udem, and M. Oglesbee.** 2002. Identification and characterization of a regulatory domain on the carboxyl terminus of the measles virus nucleocapsid protein. J. Virol. **76:**8737–8746.